Creep Failure and Fracture of Polyethylene in Uniaxial Extension

J. M. CRISSMAN *and* L. J. ZAPAS

National Measurement Laboratory
National Bureau of Standards
Washington, D. C. 20234

It is shown that under conditions of uniaxial creep the fracture of high density polyethylene can be categorized as one of three types, depending upon the magnitude of the applied load, molecular architecture, and environment. When subjected to relatively large loads, the specimens neck and then fracture almost immediately. At the other extreme of very small initial loadings, the specimens fracture in a brittle fashion through crack formation and growth. In the intermediate range of loadings the specimens neck and, depending upon the molecular weight and molecular weight distribution, may then elongate substantially before fracture. It is shown that the uniaxial creep behavior for the region where drawing occurs, when plotted in terms of isochrones, represents a type of phase diagram, one boundary of which describes the fracture envelope. In addition, experiments employing different constant rate of loading histories are described and an additivity of damage criterion used to predict the time to failure under constant load conditions, and visa versa.

INTRODUCTION

It is well known that bars of semicrystalline polymers subjected to uniaxial creep under dead loading will break if given sufficient time. In fracture mechanics, this phenomenon is known as dead load fatigue. In the case of polyethylene the ultimate fracture can be categorized as one of three types, depending upon the magnitude of the applied load, temperature, molecular architecture (molecular weight, molecular weight distribution, crystallinity, and morphology), and environment. In the present work, we shall concentrate only on the behavior in air for two high density polyethylenes of different molecular weight distributions. In general, specimens of linear polyethylene, when subjected to relatively large loadings, neck and then break almost immediately. At the other extreme of very small initial loadings, the specimens fracture in a brittle fashion through a mechanism of crack formation and growth where the deformations at fracture may be as small as 5 percent and below. In the intermediate range of loadings, it will be shown in the Results and Discussion Section that, depending upon the molecular weight and molecular weight distribution, the specimens elongate substantially before fracture occurs. The phenomenon of necking has been described by the authors (1) as a consequence of an instability which, for one high density polyethylene, occurred at a strain of around 12 percent. In the present paper, it will be shown that this behavior applies more generally to high density polyethylenes of different molecular weight.

EXPERIMENTAL

Two types of linear high density polyethylene were used which we shall designate as samples A and D. Both had a number average molecular weight (M_n) of about 15,000-16,000, however, sample A had a weight average molecular weight (M_W) of 160,000 while sample D had an M_W) of 99,000. Flat sheets of both types of polymer were compression molded and were allowed to slow-cool in the press to room temperature. The specimen densities did not differ significantly, both having values of 0.970 g/cm^3. Dumbbell shaped specimens were cut with a die and the creep strain was measured between fiducial marks placed on the straight portion of the specimen. For measurements at large loads, creep data were obtained using a hydraulically activated test machine and the strain was monitored with an extensometer (2). Several constant rate of loading experiments were also carried out by attaching a pail to the free end of the specimen and allowing water to flow into the pail at various known rates. The time to break and load at break were recorded. All of the above mentioned experiments were also carried out at several elevated temperatures in air, where the temperature of the air surrounding the specimen was controlled to within 0.1K.

Experiments to determine the Young's modulus of several specimens of the highly elongated material were performed. For this purpose, long strands of the most uniformly drawn material were chosen in order to minimize variations in area and draw ratio over the length of the strand. The modulus was determined

either dynamically in flexure or by placing a small weight on the free end of the strand and observing the amount of deformation with a cathetometer.

RESULTS AND DISCUSSION

All of the experimental results to be discussed, unless otherwise noted, were obtained in uniaxial strain histories. Creep experiments under constant load were performed on the two samples of linear polyethylene A and D and the times to fail or fracture were recorded. In the results to be described, we shall use the expression time to fail to mean the time at which the specimen necked. The reason for this terminology will be apparent as the discussion proceeds.

In *Fig. 1*, we show on a double logarithmic plot the time to fail or fracture vs engineering stress for both samples. The data, which were obtained at 296K, show little variation between the two samples. With Roman numerals, we distinguish three regions. In region I the specimens neck and break almost immediately. In region III, which corresponds to small stresses, the specimens crack and then fracture. In this region, the specimens are strained only to small deformations of the order of 5 percent and below. In region II, on the other hand, the specimens neck and then, depending upon the molecular weight and molecular weight distribution, may draw substantially to relatively high draw ratios before breaking. In *Fig. 1*, the times to fail for sample A in region II correspond to the time to neck, whereas for sample D the data shown essentially represent both necking and fracture since the specimens broke almost immediately upon necking.

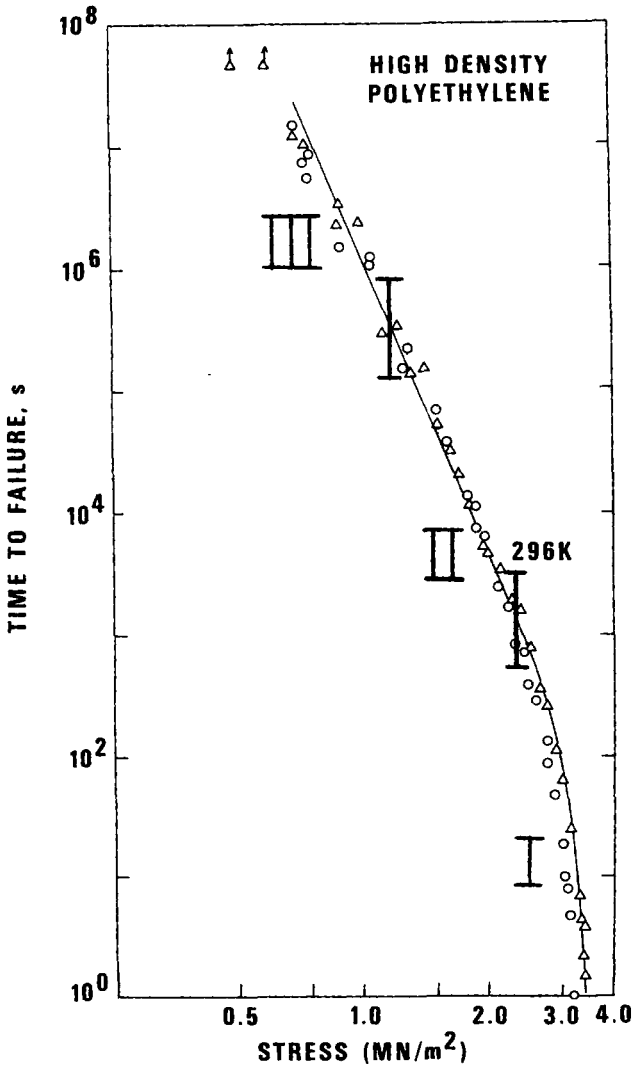

Fig. 1. Log time to failure in uniaxial extension vs log stress for two samples of high density polyethylene: circles—sample A (M_w = 160,000), triangles—sample D (M_w = 99,000). The points with arrows represent specimens still under test.

In another work (1) the authors have shown the existence of a possible instability which can be considered the precursor to the phenomenon of necking. With the use of a constitutive equation of the BKZ type (1), which properly describes the behavior of the two samples for various histories in uniaxial extension, it was shown that a critical point occurs at around 12 percent extension when a specimen is subjected to a constant load uniaxial creep deformation history. On the further assumption that the mechanisms leading to this point continue up to necking, the following condition was obtained:

$$t_f(\sigma) = \Omega\, t_c(\sigma) \qquad (1)$$

where $t_f(\sigma)$ and $t_c(\sigma)$ are the time to fail (neck) and time to reach the critical point under a stress σ, and Ω is a constant. In *Fig. 2* is given a plot of $\log t_f$ vs $\log t_c$ at 296K. In this plot the critical time t_c has been determined from the point at which the creep strain is 12 percent and it can be seen that the condition described by *Eq 1* is reasonable. The solid line represents a line of slope unity and the constant Ω is 1.85.

Constant rate of loading experiments were done on sample A by using the method outlined earlier. Care was taken to support the empty pail prior to the start of each

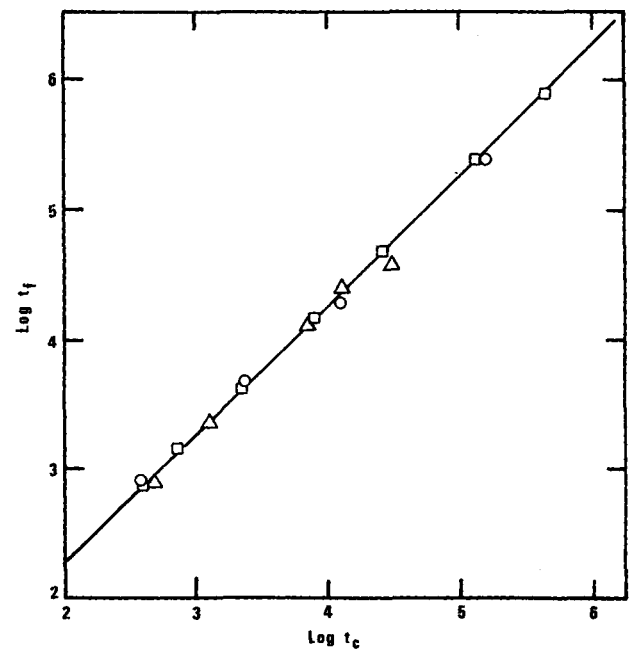

Fig. 2. Log time to failure (t_f) vs log of the critical time (t_c) at 296K: triangles–sample D (M_w = 99,000), circles–sample A (M_w = 160,000), and squares—a third linear polyethylene (not described in the text) with an M_w = 192,000 but same M_n as the other two samples.

experiment so that the stress history could be described by the following conditions:

$$\begin{aligned} &\text{For } \tau < 0,\ \sigma(\tau) = 0 \\ &\tau \geq 0,\ \sigma(\tau) = \sigma_0 + K\tau \end{aligned} \tag{2}$$

where τ is time, σ_0 is the stress due to the pail empty, and K is the rate of loading $d\sigma/d\tau$. We assume an additivity of damage criterion of the form

$$1 = \int_0^{t_b} \frac{d\tau}{\tau_b[\sigma(\tau)]} \tag{3}$$

where now $\tau_b[\sigma(\tau)]$ is the time at which the specimen would break for a dead load type of experiment under an initial stress σ as shown in *Fig. 1*. For the conditions given in *Eq 3* the following expression is obtained:

$$t_b\left(1 + \frac{\partial \ln t_b}{\partial \ln K}\right) = e^{f(\sigma_0 + \sigma_b)} \tag{4}$$

In this equation t_b is the time to failure, σ_b is Kt_b, and $f(\sigma_0 + \sigma_b)$ is the function that describes the $\log_e$ time to break vs applied stress behavior for constant load experiments. If we write

$$e^{f(\sigma_0 + \sigma_b)} = \hat{t}_b \tag{5}$$

where $\hat{t}_b$ represents the time to fail for a constant load of $(\sigma_0 + \sigma_b)$, then *Eq 4* becomes:

$$\frac{\hat{t}_b}{t_b} = \left(1 + \frac{\partial \ln t_g}{\partial \ln K}\right) \tag{6}$$

From a series of experiments conducted at different rates of loading at 296 and 330K it was found that $\partial \ln t_b/\partial \ln K$ was a constant. At 296K the value was -0.924, whereas at 330K it was -0.879. From *Eq 4* the function $f(\sigma_0 + \sigma_b)$ was then calculated for different values of its argument and the results are shown in *Fig. 3*. The lines represent the data from constant load experiments, and the circles the calculated values from the constant rate of loading experiments. The agreement is indeed remarkable considering that the problem was approached from its weakest point, that is the calculation requires evaluation of the derivative $\partial \ln t_b/\partial \ln K$. If one proceeds the opposite way, by using the data from constant load experiments, to predict the behavior under constant rate of loading, the values obtained are well within the scatter of the experimental data. In *Fig. 4*, we show the predicted time to failure vs the observed time for sample A at 296 and 350K. It should be pointed out that in a constant rate of loading experiment the time to neck is essentially also the time to break. It is for this reason that we choose to define failure as the time at which necking occurs.

In *Fig. 5* are shown the data for conditions of dead loading at several different temperatures, where the data used to calculate the predicted times to failure in *Fig. 4* were obtained using the values along the solid lines. The solid points in *Fig. 5* correspond to the times where after the material had necked, the specimens fractured. The data corresponding to the solid points were not used in the calculation for the results given in *Fig. 4*.

In region III at small loads the specimens fracture without necking. The deformation at fracture is typically of the order of 5 percent and below. As an example, we show in *Fig. 6* the creep strain as a function of time for behavior characteristics of sample D. One can observe that at the smallest loads employed, the specimens experience a nearly constant deformation for about 90 percent of its total lifetime. It is in this region where the material can be treated with a failure mechanism of the type proposed by Coleman (4). From preliminary re-

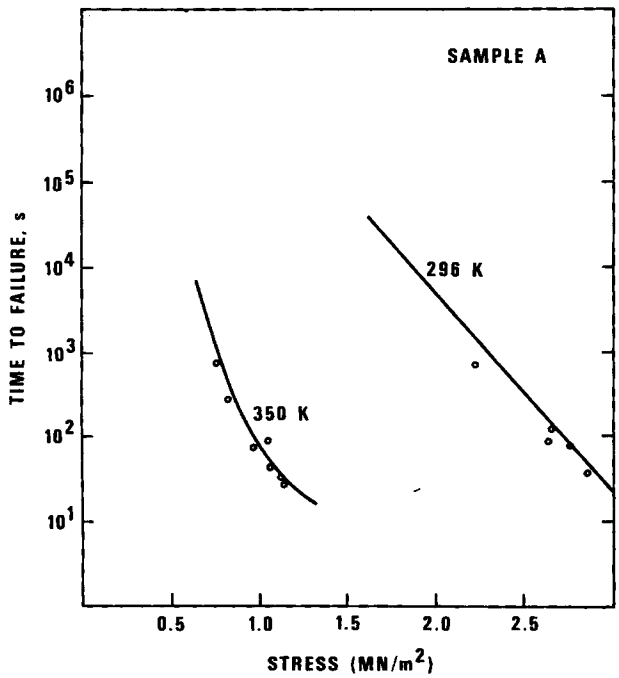

Fig. 3. Prediction of time to failure for a static load based on constant rate of loading experiments. Solid lines represent data for time to fail vs static load; circles—predicted values calculated from Eq 6.

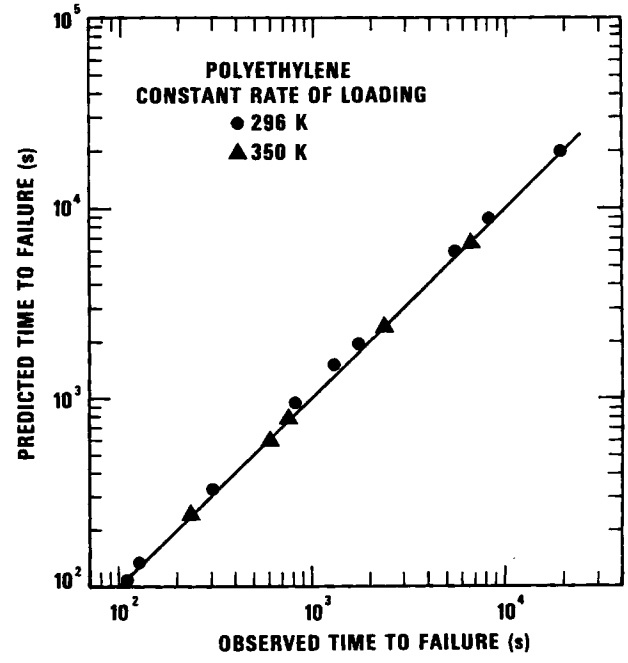

Fig. 4. Prediction of log time to failure at constant rate of loading (based on constant load data) vs log observed time to failure for sample A at two different temperatures. The solid line corresponds to a slope of unity.

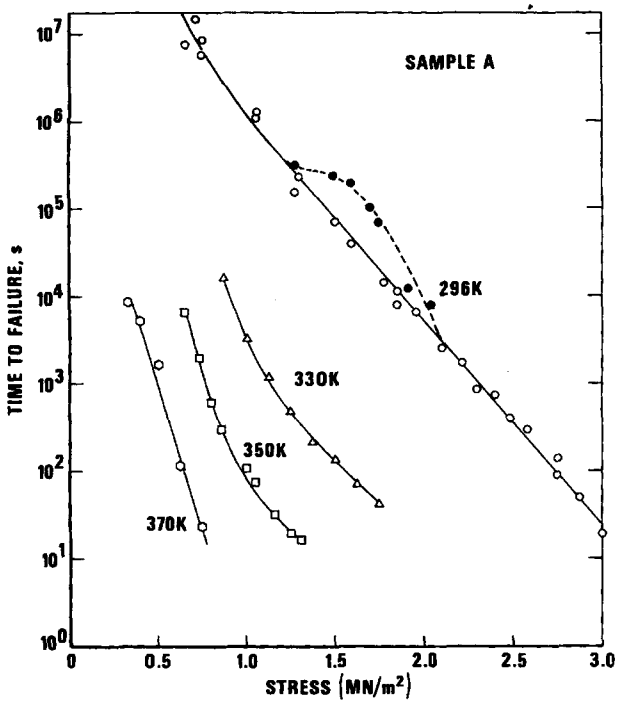

Fig. 5. Log time to fail vs applied stress for sample A. The solid points at 296K correspond to the time to fracture after necking has occurred.

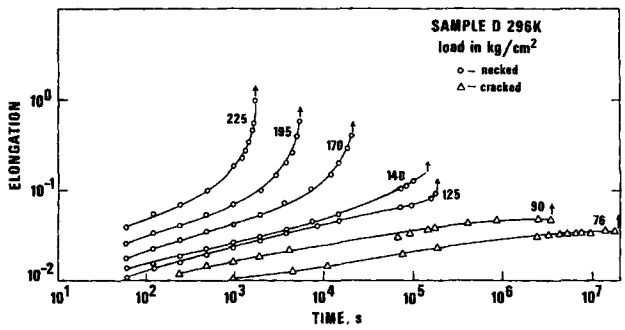

Fig. 6. Log elongation vs log time from creep measurement on sample D. The arrows indicate failure.

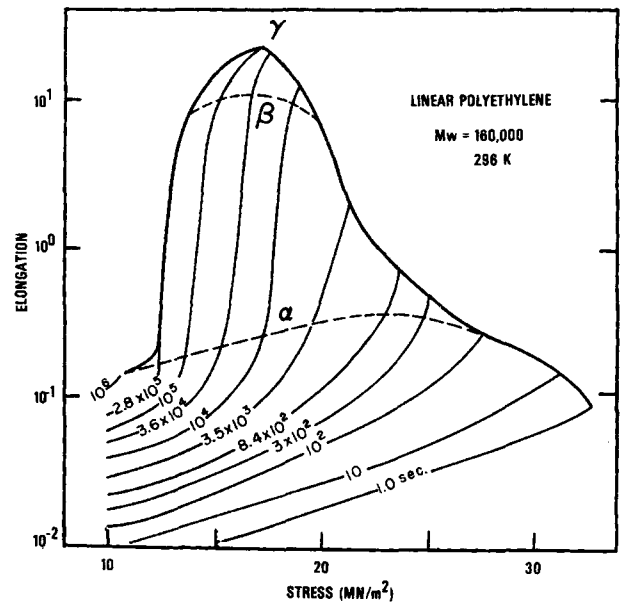

Fig. 7. Log elongation vs applied stress in terms of isochrones for the uniaxial creep of sample A. For an explanation of lines α, β, and γ, see the text.

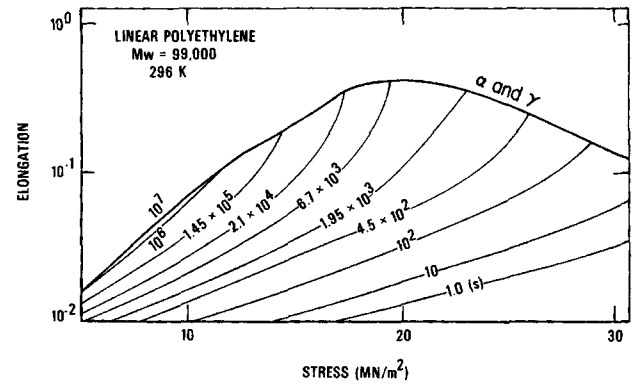

Fig. 8. Log elongation vs applied stress in terms of isochrones for the uniaxial creep of sample D. For an explanation of lines α and γ, see the text.

sults from biaxial experiments in air and uniaxial creep both in air and in adverse chemical environment, it appears possible to separate out one unique mechanism with its own activation energy which describes region III.

In an unpublished work, Bernstein and Zapas have shown that the work of Ericksen (5) on elastic bars can be extended to time dependent materials. Following their ideas, we have plotted in *Figs. 7* and *8* the creep data for samples A and D as isochrones. In *Fig. 7*, one can distinguish three distinct regions (not to be confused with regions I, II, and III shown earlier in *Fig. 1*). Line γ corresponds to the overall fracture envelope. The region underlying the dashed line α contains the region where the specimens deform homogeneously. The line α itself represents the locus of points at which necking occurs. Between lines α and β the specimens show both drawn and undrawn behavior, where line β now is the locus of points at which the neck has propagated completely through the specimen. In the small region lying between lines β and γ the deformation of the drawn material is again nearly homogeneous. Note that upon reaching the line β the specimen has deformed to a draw ratio of about 10, whereafter creep continues until a maximum elongation of about 25 is achieved. For sample A the maximum draw at 296K occurred at a load of about 165 kg/cm^2. One may consider *Fig. 7* to be a phase diagram where in the region between α and β two phases are present, one drawn and one undrawn.

For several specimens taken from the highly drawn region between β and γ the Young's modulus was determined at room temperature (296K). This was accomplished by placing a small weight on the free end of a long strand of material and measuring the elongation with a cathetometer. For specimens drawn to a draw ratio of $\lambda \simeq 21$ the modulus was found to be typically between 45 and 50 GPa. However, this value represents a lower bound since even at the smallest loadings where the strain was of the order of 2×10^{-4} the behavior was found to be nonlinear. Shorter specimens were then cut from the initially drawn material ($\lambda = 21$) and were further subjected to creep at a temperature of 360K

(87°C). A final draw ratio of about $\lambda = 36$ was achieved before the specimens broke. The modulus of the redrawn material, as determined in flexure since the specimens were too short to measure in extension, was 56 GPa, which, again, represents a lower bound of the Young's modulus.

By way of comparison, we see in *Fig. 8* that both the regions between α and β and β and λ are absent in sample D, the lower molecular weight sample. Since the primary difference between samples A and D is one of molecular weight distribution we attribute the behavior of sample A to the presence of the high molecular weight end of the distribution. This result is in agreement with the model suggested by Peterlin (6, 7) where tie molecules play a significant role in the highly drawn state permitting the lamellae to deform into a fibrillar structure at room temperature. Preliminary work on a linear polyethylene of a higher weight average molecular weight (M_w = 192,000), but approximately the same number average molecular weight indicate that the breadth of the regions between α and γ is much greater.

It is interesting to observe from *Figs. 7* and *8* that the strain at which necking occurs (line α) varies with respect to load, going through a maximum, while the critical point was taken as a constant equal to 12 percent for both samples. The time at which necking occurs, as calculated from *Eq 1*, is in excellent agreement with the experimental data, as was shown in *Fig. 2*. It should be emphasized that the critical point, or instability, should not be confused with the locus of the point at which necking occurs given by line α in *Fig. 7*. Finally, for a different strain history deformation, such as constant rate of clamp separation, the diagrams corresponding to those shown in *Figs. 7* and *8* will be different.

In conclusion, the main purpose throughout this work has been to delineate the various modes of failure which can occur in uniaxial creep experiments on semicrystalline polymer such as linear polyethylene. The usual fracture mechanics approach is applicable only in region III, where crack initiation and growth is the dominant failure mechanism. In region I one can approximate the behavior as a ductile fracture. In region II there is no appropriate description for fracture since extensive drawing can occur depending upon the chemical architecture of the polymer. The idea of accumulative damage has been employed successfully for experiments where the strain is monotonically increasing. Additional experiments, not reported here, with other strain histories have also yielded encouraging results. It is our intention in the future to direct further attention toward this point. The idea of describing the creep behavior in terms of isochrones shows, in a sense, the existence of two phases, and provides a compact representation of the failure envelope for necking (line α), the envelope for fracture (line γ), and the locus of points (line β) corresponding to what is generally referred to as the natural draw ratio.

REFERENCES

1. L. J. Zapas and J. M. Crissman, *Polym. Eng. Sci.*, **19**, 104 (1979).
2. The authors are indebted to Dr. R. W. Penn of our Laboratory for performing the rapid creep experiments on the hydraulic test machine.
3. B. Bernstein, E. A. Kearsley, and L. J. Zapas, *Trans. Soc. Rheol.*, **7**, 391 (1963).
4. B. D. Coleman, *J. Polym. Sci.*, **20**, 447 (1956).
5. J. L. Ericksen, *J. Elasticity*, **5**, 191 (1975).
6. A. Peterlin and G. Meinel, *J. Polymer Sci. B*, **3**, 783 (1965).
7. A. Peterlin and G. Meinel, *J. Polym. Sci. B*, **5**, 613 (1967).